20th Australasian Fluid Mechanics Conference
Perth, Australia
5-8 December 2016

Duty cycle effect on jet control based on a single unsteady minijet

Cao H L[1,2], Perumal A K[2], Bai L[2], Fan D W[2], Zhou Y[2]
[1] State Key Laboratory of Aerodynamics , China Aerodynamics Research and Development Center,Mianyang Sichuan 621000,China
[2] Institute for Turbulence-Noise-Vibration Interaction and Control
Harbin Institute of Technology, Shenzhen Graduate School, Shenzhen, 518055, China

Abstract

An experimental investigation has been carried out to assess the mixing promoting capability on a turbulent round jet of Reynolds number 8000 controlled by a single unsteady radial minijet. The influence of the duty cycle d_c of the unsteady minijet on jet mixing characteristics has been investigated. The decay rate K of the jet centerline mean velocity is strongly influenced by the duty cycle. Moreover, the optimum duty cycle increases with increasing C_m. The increase in duty cycle is closely linked to the depth of the minijet penetration and the generation of mush-room-like structures, resulting in greatly enhanced jet mixing. Flow visualization results reveal that at small C_m the unsteady injection can only affect the shear layer and suppress the vortex-pairing on the injection side, thus resulting in the jet column to flap. However, at larger C_m the unsteady injection may have penetrated the main jet, causing a highly turbulent jet, irrespective of d_c .

Introduction

The fundamental understanding and control of round jets have been of great interest over the years, due to their applications in many fields of engineering, such as combustor, chemical process, thrust vector control, reduction in infrared-signature, etc. Many studies have been reported in open literature, for the jet controlled using active and passive methods. These methods primarily aim, to affect the flow structure in the jet, which results in jet mixing with the ambient fluid. The passive controls, such as tabs located at the nozzle exit, non-circular nozzles, require no energy into the flow and are very attractive due to their simpler implementation and lower cost. However, these techniques carry with them certain penalties (weight, thrust loss, drag, practical constraints, etc.). On the other hand, active techniques inject energy into the flow via imparting controlled perturbations to the jet near the jet vicinity, such as acoustic excitation, synthetic jets, plasma actuators, and steady/unsteady jets. In recent years, unsteady or pulsed jets injection is one of the efficient controlling technique, because they can be easily adapted to the flow conditions and will not cause thrust loss; additionally, the penalty in increased weight, cost, and mechanical complexity is also reduced.

Pulsed jet injections are more effective than the steady injection[1], because the unsteady injection is associated with a deeper penetration into the potential core. Also, the periodic excitation of jet instabilities may capitalize not only on large-scale changes through penetration but also on the excitation frequency to manipulate the inherent instabilities of the main jet. Zhang [2] studied in detail on the control of a turbulent round jet using two symmetrically arranged radial unsteady minijets and identified three types of coherent structures, i.e. the distorted vortex ring, two pairs of azimuthally fixed streamwise vortices and sequentially ejected mushroom-like counter-rotating structures. Yang *et al*., [3] expanded the study of Zhang [2], using two radial unsteady minijets separated azimuthally by 60 degrees and found that flapping motion was responsible for the substantial increase in jet spread, thus giving rise to rapid decay of the centerline velocity. Kamran and McGuirk [4] carried out numerical study on mixing enhancement with pulsed control jets in symmetric and antisymmetric modes, on a high Reynolds number and high subsonic Mach number (Re = 10^6, M = 0.9), at the duty cycle of 0.32 and observed the flapping behavior for the antisymmetric case, whereas no such behavior was observed for the symmetric case. Most of the studies were restricted to the research of preferred excitation frequency and mass flow rate of the minijets to achieve optimal performances. For pulsed minijets, an additional parameter is available for system optimization, namely the duty cycle (d_c), the percentage of time the minijet is "on" during each pulsation cycle. Annaswammy *et al.*, [5] addressed that the duty cycle and pulsing frequency have the most dominant effect on the jet noise as well as on the overall flow field. Ragaller *et al.*, [6] reported that, at a given injection pressure the noise reduction increases with increasing duty cycle. However, little study has been done on the effect of duty cycle on jet mixing enhancement. Naturally, questions arise. Is it highly effective? If yes, what's the reason behind it and is there any change in flow behaviour? These issues fascinating and motivate the present investigation.

Experiments have been carried out in a round turbulent jet under the excitation of a single unsteady minijet. In order to address the effect of duty cycle on jet mixing enhancement, the main jet was controlled using a single unsteady minijet, in the duty cycle range of 5-100%, were the 100% corresponds to steady injection. Hot-wire and flow visualization measurements were conducted to study the influence of duty cycle on jet mixing characteristics. This paper first presents the results of jet centerline velocity decay rate variation with mass flow ratio of minijet to the main jet, at fixed duty cycle of 15%, and as a result, two optimum conditions (C_m) are obtained. Then we further study the dependence of jet decay rate on the duty cycle at two given C_m. Finally, typical flow visualization results in both the injection and non-injection plane are presented to explain the flow physics.

Experimental details

Experiments for the present study were performed at Harbin Institute of Technology Shenzhen Graduate School, Shenzhen, China. The test facility consists of a main-jet and minijet assemblies as shown in Fig. 1. Compressed air passes through a mixing chamber, mixed with seeding particles in the case of flow visualization, and a plenum box, consisting of 300-mm-long diffuser of 15° in half angle, before entering the settling chamber of 400 mm in length. A nozzle with 114 mm inner diameter and an outer diameter of 20 mm is fitted to the end of the settling chamber. The profile of the nozzle contraction is given by $R = 57 - 47\sin^{1.5}(90 - 9x/8)$, as used by Mi *et al*., [7]. The

nozzle was extended with a 47-mm-long smooth tube of diameter 20 mm. The minijet includes an electromagnetic valve group (6 valves) in which each valve can be independently controlled. The nozzle was drilled with six holes of 1mm diameter, separated azimuthally by 60 degrees, and located 17 mm upstream of the main jet exit. Each hole is connected via short plastic hose to an electromagnetic valve (Koganei K2-100SF-09-LL) with its maximum frequency of 1kHz, generating unsteady minijet. In this study, only a single minijet was used (marked with No.2 in Fig.1b). The valve was driven by the modified voltage signal (0 - 5 V square wave signal). Both the frequency and duty cycle can be adjusted by changing the frequency and duty cycle of the output square wave signal from the output board of a NI system. The mass flow rates of the main jet and minijet were measured by two flow meters, whose experimental measurement uncertainties were less than 1%. The main jet Reynolds number Re_D is 8000 based on the jet exit velocity and nozzle exit diameter. The dimensionless parameter C_m is defined as the mass flow ratio of the minijet to main jet, and f_e / f_o is the ratio of the excitation frequency f_e to the preferred-mode frequency f_o.

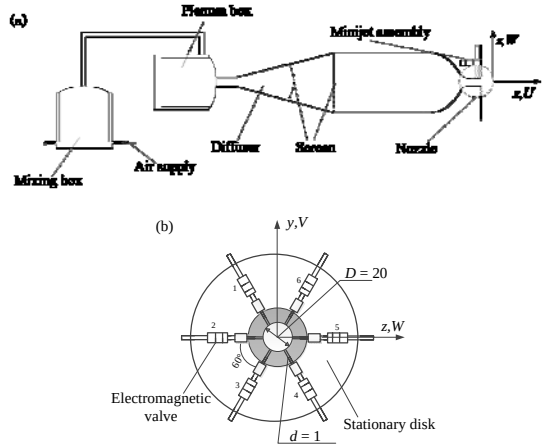

Figure 1 Schematic of experimental setup: (a) main-jet assembly; (b) minijet assembly.

The coordinate system is defined in such a way that its origin is at the centre of the nozzle exit, with the *x* axis along the streamwise/jet direction, the *z* axis along the opposite side of minijet injection, i.e, -*z* direction is aligned with the minijet injection and *y* axis along the direction perpendicular to (*x*, *z*) plane, following the right-hand system. The (*x*, *z*) and (*x*, *y*) planes are referred to as the injection and non-injection planes, respectively.

The streamwise velocity was measured using a single calibrated hotwire probe, operated on a constant temperature circuit (Dantec Streamline) with an overheat ratio of 0.6. The voltage signal from the hot-wire was filtered using a low-pass Gaussian filter at a cut-off frequency of 3 kHz, amplified 8 times and then digitized using a 16-bit A/D board (NI USB-6361) at a sampling frequency of 6 kHz. The duration for each record was 80s. The uncertainty of the hot-wire measurement has been estimated to be less than 2%.

Flow visualization measurements in the injection and non-injection planes, were carried out using a planar PIV (Dantec SpeedSence 90C10). A TSI oil droplet generator (TSI MCM-30) was used to generate fog for the seeding of flow. The particles were supplied into the mixing chamber (Fig.1 a), mixing with air and fully spread throughout the main jet. Flow illumination was provided by a Litron LDY300 laser with 527 nm in wavelength and a maximum energy output of 30 mJ per pulse. Particle images were captured at a sampling rate of 600 Hz. The synchronization of the flow illumination and image capturing was controlled by Dynamic studio (v3.41). The capture images covered an area of *x/ D* = 0 ~ 6 and *y/ D* or *z/ D* = -2 ~ 2 in (*x*, *y*) and (*x*, *z*) planes. Also a series of cross-sectional (*y*-*z*) flow visualization was conducted up to five nozzle diameters in the downstream direction of the jet exit.

Results and discussion

In general, the performance of the unsteady minijet injection is strongly influenced by number of minijet injected, its geometric arrangement, exit diameter, angle of injection with respect to the main stream flow, the mass flow ratio, excitation frequency, duty cycle, etc. These parameters should be carefully chosen for optimizing performance. In this work, the effect of duty cycle on jet mixing was investigated in order to provide a database for further close-loop control study. The main jet velocity was fixed at 6 m/s, and its corresponding preferred-mode frequency was 135 Hz (Figure not shown), corresponding to a Strouhal number of $St_D = f_0 D / U_e$ = 0.45, falling in the range (0.24-0.64) previously reported by Gutmark and Ho[8]. Following Zhou *et al.*, [9], the jet centreline decay rate *K* was used to evaluate jet mixing, given by $K = (U_e - U_{5D}) / U_e$, where U_e and U_{5D} are the mean jet centreline velocity at *x/D* = 0 and 5, respectively.

Dependence of jet decay rate on C_m

Figure 2 shows the variation of decay rate *K* with the ratio of mass flow rate at duty cycle of 15% and f_e / f_o = 1. For comparison, the results of natural jet is also shown. There are two distinct peaks, the first one occurs at C_m = 0.19%, and the other one at C_m = 2.31%. The decay rate (0.248) at C_m = 0.19% is smaller than that (0.383) at C_m = 2.31%. These two peaks may result from different mixing mechanisms, which will be further discussed from flow visualization results.

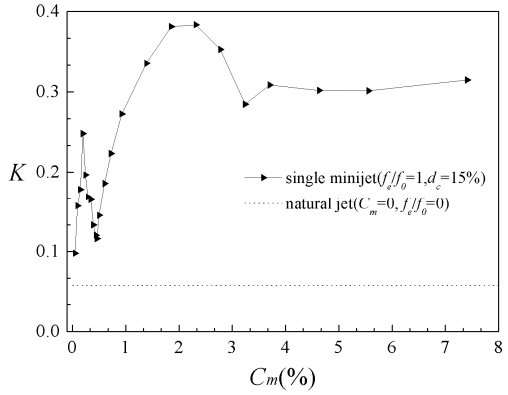

Figure 2 Dependence of *K* on C_m at duty cycle of 15%

The penetration of unsteady minijet into the main jet is closely related to the momentum of unsteady injection. The optimal control performance is to optimize minijet penetration and enable maximum interaction between minijet flow and main jet. When the mass flow rate of radial minijet is relatively small, the momentum is not large enough to penetrate the main jet core region, the effect of radial injection are only imposed upon the jet shear layer in the vicinity of the minijet. When the mass flow rate increases, the radial injection can penetrate sufficiently deep into the jet cores and even further downstream, thereby the turbulence level increases (not shown here). Therefore, the effect of duty cycle may behave different since the underlying flow phenomenon is different at different C_m. The other reason is that, a smaller mass flow rate of minijet is more preferable from the

point of view of its practical applications. Therefore, in the following part we focus on these two C_m to investigate the effect of duty cycle.

Dependence of jet decay rate on duty cycle

The unsteady minijet was operated in a range of d_c = 5% - 100%, where d_c = 100% corresponds to steady injection. Figure 3 presents the dependence of the jet centreline decay rate *K* on the duty cycle at $f_e / f_o = 1$ for two C_m. A local *K* maximum (0.248) occurs at duty cycle d_c = 15% for small C_m (= 0.19%), while another minor peak occurs at duty cycle d_c = 45%, after that the *K* variation flattens out. With increasing C_m to 2.31%, the optimum duty cycle shifts to 40% and gives rise to maximum *K* (0.506). Note that at the duty cycle 100% (steady injection) achieves the same *K* as at d_c = 15%.

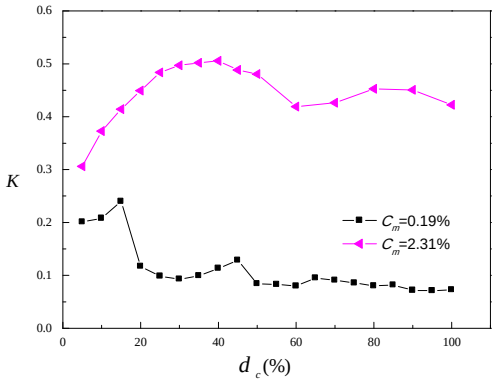

Figure 3 Dependence of *K* on duty cycle at $f_e / f_o = 1$

Effect of duty cycle on flow structure

In this section, the flow structures under typical excitation conditions are considered, to understand the physics behind the effect of C_m and d_c on the jet decay rate. Figure 4 shows the typical flow visualization results for C_m = 0.19% (d_c = 15% and 45%) and 2.31% (d_c = 15% and 40%) in the injection and non-injection planes. For reference, the flow structure for uncontrolled case is also given. It can be observed that the uncontrolled jet (Fig. 5a) remains stable until 1.5*D*, and then the shear layer instabilities finally set in. This causes small-scale vortex roll-ups to manifest and the jet column transit to turbulence after three cycles of vortex roll-ups.

With radial minijet discernible flow difference can be detected in the near field region. Note that the minijet injection is from top to bottom. Compared with uncontrolled jet, the inception point of the vortex roll-ups occurs much nearer to the jet exit. At small C_m (= 0.19%, d_c = 15%), the perturbed shear layer begins to roll up into vortices at 0.6*D* and large-scale structures become more turbulent and break down to fine structure turbulence after two or three cycles of vortex roll-ups (Fig. 4c1). It should be noted that the vortex-paring process on the side of radial injection is suppressed. At this C_m, the minijet had not penetrated the jet core, evident from the asymmetric jet structure in the injection plane (Fig. 4b1 and 4c1). Since, the minijet had not penetrated the main jet core, the shear layer begins to roll-up into vortices at 1.2*D*. In other words, the roll-up of shear layer in the injection side is much earlier than the non-injection side, which is due to the minijet injection. This leads to the formation of asymmetric jet structure, results in the jet column to oscillate. Such an oscillation of the jet structure is referred as flapping jet column, as observed by Yang *et al*., [3]. The flow structure in the non-injection plane (Fig. 4c2) is still symmetric, and entrainment of ambient fluid into the main jet core can be observed around 1*D*.

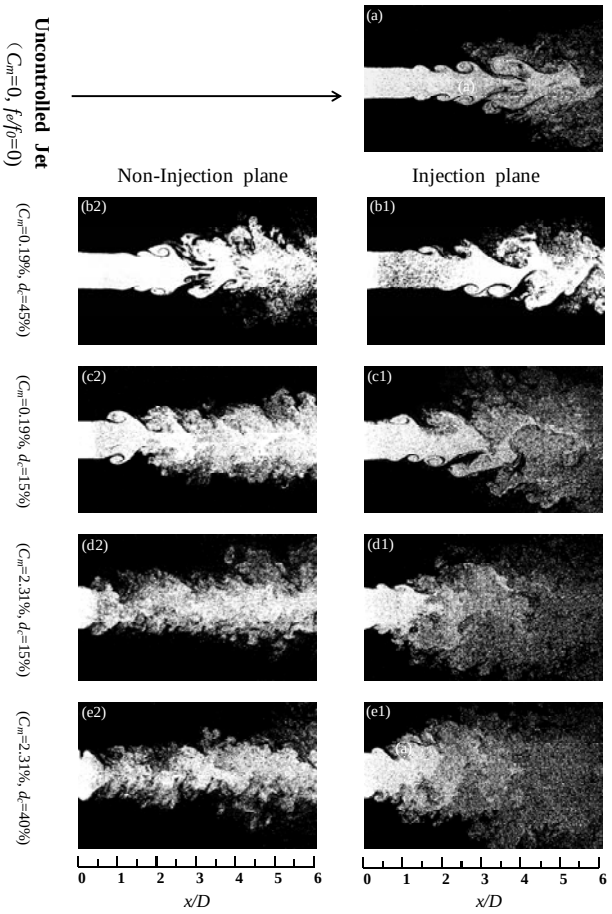

Figure 4 Photographs of typical flow structures from flow visualization

With increase C_m to 2.31% (d_c = 15%), the presence of large-scale vortex roll-ups is no longer detected. Instead, apparently the great momentum of minijet penetrates into the main jet core causes small-scale vortex roll-ups (in both injection and opposite side of injection) adjacent to the nozzle exit (Fig. 4d1), which occurs very close to jet exit than before. Compared with Fig.4 (c1), the main jet column seems turbulent, which suggests that with increasing mass flow ratio, the radial minijet penetrate deeper into the main jet. Not surprisingly, further increasing in C_m, the main jet will become largely incoherent and turbulent.

At C_m = 2.31% (d_c = 40%), the vortex structure remain coherent at least in the vicinity of nozzle exit (Fig. 4e1). Compared with Fig. 4(d1), instead of two small adjacent vortices, a larger vortex structure can be observed near the nozzle exit, due to high duty cycle enforce a strong impingement (per pulse) upon the jet core region. Note that larger spread in the *z* direction compared to the *y* direction for both cases. Compared with Fig.4 (d2) and 4(e2), it seems the entrainment of ambient fluid into main jet core is enhanced for the latter case (d_c = 40%), results in a large decay rate *K*.

In order to get an insight into the flow physics associated with the manipulated jets at C_m = 2.31% (d_c = 15% and 40%), flow visualization were carried out at various cross-sectional planes of the jets. It has been noted during careful examination of flow

visualization that the flow behaviour observed is highly repeatable. As such, we present in Fig 5, three sequential photographs at x/D = 1.0, for C_m = 2.31% (d_c = 15% and 40%). Several observations can be made. First, at both duty cycles, mushroom-like structures (Figs. 5a and 5d) begin to form along the injection and non-injection planes. Second, once formed, these mushroom-like structures grow in size by entraining the ambient fluid. The size of the mushroom-like structures is larger at d_c = 40% than at 15% (Fig. 5b and 5e). These mushroom-like structures, move outwards along the radial direction, which is accompanied by a strong ejection of jet core fluid, resulting in greatly enhanced jet mixing. Thus, the formation of mushroom-like structures implies that the jet spread is caused by the entrainment of ambient fluid [10]. Third, at d_c = 15% (Fig. 5c), the mushroom-like structures, still grows in size. Moreover, the growth of the mushroom-like structures is not that developed. Whereas, at d_c = 40% (Fig. 5f), the developed mushroom-like structure disappears, revealing that the growth to die phase of the mushroom-like structure is completed.

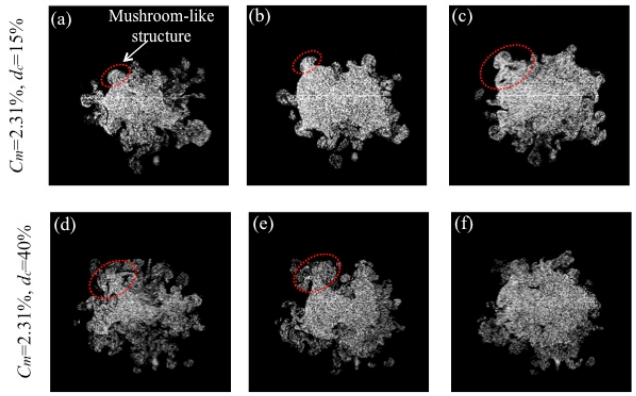

Figure 5 Photographs of typical flow structures from flow visualization at x/D = 1.0. Time interval between two successive images is 0.00166 s. Minijet Injection is from left to right.

With increase in duty cycle, the time period of the minijet injection increases and the minijet velocity decreases, during the 'on' period of the pulsating cycle. Thus, this might lead to the formation of the stronger (in size) mushroom-like structures. However, at higher duty cycle, the jet may behave similar to the steady injection case. This is because a higher duty cycle results in a reduction of spatial distance between the vortex structures of the minijet, and vortices will have less time to interact with the main jet structures independently, thus behaving quasi-steady, resulting in a drop in the decay rate (Fig. 3).

The reason for the increased decay rate at d_c = 40% than 15%, is two folds. First, at d_c = 40%, the minijet injection results in the formation of stronger (in size) mushroom-like structures. Second, at d_c = 40%, these mushroom-like structures find sufficient time to grow, interact with the main jet and then die, thereby promote mixing. Whereas, at d_c = 15%, the growth of the mushroom structures, its interaction with the main jet and then die, phases are absent.

Conclusions

Experimental investigation has been carried out to assess the performance of single unsteady minijet in the manipulation of a turbulent round jet at Reynolds number 8000. Emphasis has been placed on understanding the effect of the duty cycle on jet mixing. Hot-wire and flow visualization measurements are performed in the injection and non-injection planes of the controlled jet. It has been found that the jet centerline mean velocity decay rate is strongly dependent on d_c . Moreover, the optimum duty cycle increases with increasing C_m. Following conclusion can be drawn from the present investigation.

At small C_m unsteady injection can only affect the shear layer, resulting in the formation of asymmetric jet structure and even the oscillation of the jet column, i.e. jet column flapping, and hence jet mixing enhancement.

The optimum duty cycle depends on two phenomena. First, the velocity and time period of the minijet injection results in the formation of stronger (in size) mushroom-like structures. Second, these mushroom-like structures find sufficient time to grow and interact with the main jet before vanishing, thereby promote mixing.

At a large duty cycle, the jet may behave similarly to the steady injection case. This is because a higher duty cycle results in a reduction of spatial distance between the vortex structures of the minijet, and these vortices will have less time to interact with the main jet structures independently, thus behaving quasi-steady, resulting in a decrease in the decay rate.

Acknowledgments

The authors wish to acknowledge support from National Natural Science Foundation of China (Grant No 11402068) and support from State Key Laboratory of Aerodynamics (SKLA20140302).

References

[1] Kamran, M. A., & McGuirk, J., Subsonic Jet Mixing via Active Control Using Steady and Pulsed Control Jets, *AIAA Journal*, 2011, 49(4), 712–724.

[2] Zhang P. Active control of a turbulent round jet based on unsteady microjets. PhD Thesis, The Hong Kong Polytechnic University, Hong Kong, 2014.

[3] Yang H, Zhou Y, So, R M C, Liu Y. Turbulent jet manipulation using two unsteady azimuthally separated radial minijets. *Proceedings of The Royal Society A Mathematical Physical and Engineering Sciences* 472(2191): 20160417

[4] Kamran, M. A. & Mcguirk, J. J., Unsteady Predictions of Mixing Enhancement with Steady and Pulsed Control Jets. *AIAA Journal*, 2015, 53(5): 1262-1276.

[5] Annaswamy, A. M., Choi, J. J. & Alvi, F. S., Pulsed microjet control of supersonic impinging jets via low-frequency excitation. Proceedings of the Institution of Mechanical Engineers -- Part I, 2008, 222(5): 279-296.

[6] Ragaller, P. A., Annaswamy, A. M., Greska, B. & Krothapallli, A., Supersonic jet noise reduction via pulsed microjet injection. 15th AIAA/CEAS Aeroacoustics Conference, 11 - 13 May 2009, Miami, Florida.

[7] Mi J, Nobes D & Nathan G J., Influence of jet exit conditions on the passive scalar field of an axisymmetric free jet. *Journal of Fluid Mechanics*, 2001, 432, 91-125.

[8] E. Gutmark and C. M. Ho, Preferred modes and the spreading rates of jets, Physics of Fluids, 1983, 26, 2932.

[9] Zhou Y, Du C, Mi J, Turbulent Round Jet Control Using Two Steady Minijets. *AIAA Journal*, 2012, 50(3), 736-740.

[10] Liepmann, D. and Gharib, M. "The role of streamwise vorticity in the near-field entrainment of round jets," J. Fluid Mech. 245, 643(1992)